

QUANTITATIVE MEASUREMENTS OF DOUBLE-PHOTON ABSORPTION  
IN THE POLYCYCLIC BENZENE RING COMPOUNDS

D. H. McMahon, R. A. Soref, and A. R. Franklin

Sperry Rand Research Center, Sudbury, Massachusetts

(Received 20 May 1965)

Double-photon absorption has been observed in several polycyclic benzene ring compounds via a subsequent fluorescence decay,<sup>1-4</sup> but the mechanism by which this process takes place is not definitely established.<sup>2-8</sup> In order to clarify the mechanism, we have made quantitative measurements of the double-photon transition probability in 12 different polycyclic benzene ring compounds in both the liquid and the solid state. We observed double-photon absorption in every compound tested, including phenanthrene<sup>1</sup> and several others not previously reported. In both liquids and solids, the presence or absence of molecular inversion symmetry does not produce a dichotomy in values of the double-photon transition probability. For each compound, the magnitude of the observed transition probability is such that it can only be explained by using the Göppert-Mayer mechanism of double-photon absorption.<sup>2,6,7,9</sup>

Using the electromagnetic potential

$$H = \frac{e}{mc}(\vec{A} \cdot \vec{p}) + \frac{e^2}{2mc^2}A^2,$$

double-photon absorption can take place in first-order time-dependent perturbation theory by means of the  $A^2$  term, or in second-order perturbation theory by means of the  $(\vec{A} \cdot \vec{p})$  term. If the factor  $\exp(i\vec{k} \cdot \vec{r})$  of  $A$  is set equal to unity, the electric dipole, or Göppert-Mayer, approximation is obtained. If, by reasons of symmetry, the Göppert-Mayer mechanism cannot connect a given initial and final state, the higher order multipole contributions of the  $(\vec{A} \cdot \vec{p})$  term, obtained by expanding  $\exp(i\vec{k} \cdot \vec{r})$ , become important. An estimation of the magnitude of the transition probabilities for double-photon absorption shows that the Göppert-Mayer mechanism is about  $10^4$  times larger than either the  $A^2$  mechanism or the interactions involving the multipole expansion of the  $(\vec{A} \cdot \vec{p})$  term.

In the present experiment 20-W pulses of 6940Å light from a ruby laser were filtered and focused upon a 1.9-cm-long sample cell which contained a small amount of a given polycyclic benzene ring compound dissolved in benzene. A portion of the fluorescence excited

within the cell was collected by a lens and focused through a 7-in.-long saturated solution of copper sulfate. The signal was then detected by a calibrated S-20 photomultiplier tube and observed directly on an oscilloscope. No signal appeared if no cell was placed in the laser beam or if a cell containing only benzene was placed in the beam. For measurements in solids, thin translucent polycrystalline layers were grown from the melt between microscope slides spaced 0.07 mm apart. The diameter of the laser beam at the sample was 0.9 mm in all cases.

Since double-photon absorption is observed via fluorescence, the quantum efficiency of the fluorescence is required in order to deduce the actual absorption probability. We have attempted to take this factor into account by measuring the quantum efficiency for single-photon absorption at 3470 Å, and then applying this value to the double-photon case. The single-photon quantum efficiency would, however, be applicable only if the final state is the same at 3470 Å for both single- and double-photon absorption. Measurements were made at 3466 Å with a cadmium vapor lamp. Because the absorption bands of these molecules are typically 100 Å wide, the distinction between 3466 Å and 3470 Å is negligible.

Table I lists the results of our measurements. Here  $P_f$  is the total fluorescence power emitted by the sample divided by the number of moles of sample molecule irradiated. We define the quantity  $P_a$  by the formula  $P_a = P_f/Q$ , where  $Q$  is the quantum efficiency for single-photon absorption at 3470 Å. By using our definition of  $P_a$  and assuming that  $Q$  is the correct quantum efficiency for double-photon absorption at 3470 Å, the double-photon transition probability  $W$  is directly related to  $P_a$  by the equation  $W = P_a/N\hbar\omega$ . Here  $N$  is Avogadro's number and  $\hbar\omega$  is the double-photon energy.

Because the molar extinction coefficient is directly related to the single-photon transition probability, one might expect a correlation via the density of final states between this coefficient and the double-photon transition prob-

Table 1. Measured constants of single- and double-photon absorption at 3470 Å in 12 polycyclic benzene ring compounds. In liquid samples, benzene is the solvent,  $\epsilon$  is the molar extinction coefficient,  $Q$  is the single-photon absorption quantum efficiency measured at 3470 Å,  $P_f$  is the observed fluorescence power divided by the number of moles of sample molecule irradiated, and  $P_a = P_f/Q$ . In crystalline samples, the definitions for  $Q$ ,  $P_a$ , and  $P_f$  are the same as in liquid samples. The solution values of  $Q$  were calculated assuming unit quantum efficiency for perylene in benzene; the crystalline values were calculated assuming unit quantum efficiency for chrysene and benzanthracene.

	Molecular inversion symmetry	$\epsilon$ $10^3 \text{ cm}^2$ mole	Liquids			Solids		
			$Q$	$P_f$ (W/mole)	$P_a$ (W/mole)	$P_a$ (W/mole)	$P_f$ (W/mole)	$Q$
Anthracene	Yes	6000	0.15	0.03	0.2	3	2	0.7
Naphthacene	Yes	23	0.004	0.0008	0.3	...	...	...
Chrysene	Yes	150	0.06	0.03	0.5	0.5	0.5	1
Pyrene	Yes	2500	0.4	0.03	0.08	0.2	1.5	0.7
Perylene	Yes	1700	1.0	2	2	45	22	0.6
Dibenzanthracene	Yes	10 000	0.05	0.05	0.9	0.1	0.08	0.7
Phenanthrene	No	360	0.11	0.05	0.4	0.3	0.2	0.6
Fluorene	No	7000	0.24	0.0002	0.001	0.002	0.001	0.6
Benzanthracene	No	750	0.06	0.03	5	3	3	1
Triphenylene	No	65	0.025	0.005	0.2	0.8	0.1	0.1
Fluoranthene	No	7000	0.10	0.02	0.2	0.6	0.3	0.5
Benzopyrene	No	7000	0.2	0.09	0.4	1	0.6	0.6

ability. We have therefore measured the molar extinction coefficients at 3470 Å and have listed the results in Table I. We do not find any meaningful correlation, and attribute this result to variations in the oscillator strengths of the relevant matrix elements for the different molecules.

By comparing in Table I the liquid and crystalline values of  $P_a$  for a given molecule, we find a much larger relative change in the centrosymmetric molecules than in the noncentrosymmetric molecules. A possible explanation of this phenomenon is to attribute the larger change in centrosymmetric molecules to the inapplicability of the single-photon quantum efficiencies. The measured single-photon quantum efficiencies would, in fact, not apply if the final states for single- and double-photon absorption at 3470 Å were different. From this argument we infer that there exists, at 3470 Å in centrosymmetric molecules, states of the same parity as the ground state as well as states of opposite parity.

Finally we consider the importance of the mechanism proposed by Pao and Rentzepis<sup>3</sup> to account for double-photon absorption in noncentrosymmetric molecules. Since we have found that  $P_a$ , and hence the double-photon transition probability, is comparable in the

liquid and solid states, it does not appear likely that the absorption of second-harmonic radiation plays an essential role in producing the observed fluorescence. The intermolecular coherence necessary for the rapid buildup of second-harmonic power is not present in a random molecular arrangement.

To summarize, the double-photon transition probabilities have been measured in 12 different polycyclic benzene ring compounds in both the liquid and solid states. It was found that the magnitude of the transition probabilities are independent of molecular inversion symmetry and that the magnitudes can only be explained by using the Göppert-Mayer mechanism of double-photon absorption. From a comparison of the transition probabilities, it appears likely that the absorption of second-harmonic radiation is not the dominant mechanism of double-photon absorption in noncentrosymmetric molecules.

<sup>1</sup>W. R. Peticolas, J. R. Goldborough, and K. E. Rieckhoff, Phys. Rev. Letters **10**, 43 (1963).

<sup>2</sup>S. Singh and B. P. Stoicheff, J. Phys. Chem. **38**, 2032 (1965).

<sup>3</sup>Yoh-Han Pao and P. M. Rentzepis, Bull. Am. Phys. Soc. **10**, 393 (1965).

<sup>4</sup>P. D. Maker and R. W. Terhune, Phys. Rev. **137**,

A801 (1965).

<sup>5</sup>M. Iannuzzi and E. Polacco, Phys. Rev. Letters **13**, 371 (1964).<sup>6</sup>R. Guccione and J. Van Kranendonk, Phys. Rev. Letters **14**, 583 (1965).<sup>7</sup>W. L. Peticolas and K. E. Rieckhoff, Phys. Letters **15**, 230 (1965).<sup>8</sup>M. Iannuzzi and E. Polacco, Phys. Rev. **138**, A806 (1965).<sup>9</sup>M. Göppert-Mayer, Ann. Physik **9**, 273 (1931).

## CYCLOTRON RESONANCE ECHO\*

R. M. Hill and D. E. Kaplan

Lockheed Research Laboratories, Palo Alto, California

(Received 17 May 1965)

We have observed strong echoes radiated from a partially ionized gas plasma following excitation by a sequence of short pulses at the electron cyclotron resonance frequency. These signals have been observed only when the exciting microwave radiation is propagating perpendicular to the magnetic field, and have decay constants which we believe are determined by the electron relaxation processes in the plasma.

The simplest example of an electromagnetic echo is the two-pulse echo. A system consisting of a large number of resonators is excited by a short intense pulse of radiation, followed at a time  $\tau$  by a second pulse. The second pulse triggers the coherent emission of part of the stored energy as an echo pulse which is radiated at the interval  $\tau$  after the second pulse (Echo I, Fig. 1). The two-pulse-echo decay constant is observed by increasing  $\tau$  and noting the rate at which the echo amplitude decreases. A three-pulse stimulated echo is obtained when a third radiation pulse is applied at some time  $T$  after the first two pulses. The stimulated echo is observed at the interval  $\tau$  after the third pulse and its amplitude (Echo II, Fig. 1) is a function of both  $T$  and  $\tau$ . The stimulated-echo decay constant is found by varying  $T$  alone. Echoes were first observed for nuclear para-

magnetic resonance,<sup>1</sup> and subsequently from electron spin resonance,<sup>2</sup> optical transitions in atoms,<sup>3</sup> and ferrimagnetic resonance.<sup>4</sup> Our resonant system consisted of the free electrons in an afterglow plasma, immersed in a slightly inhomogeneous magnetic field. The plasma was produced by ionizing a gas, Ar, Ne, or N<sub>2</sub>, contained in a rectangular, glass bottle with a pulsed 21-Mc/sec transmitter. The X-band microwave apparatus was similar to that used for the ferrimagnetic echo experiment.<sup>4</sup> The glass bottle replaced the cavity and was illuminated by microwave horns designed to produce plane waves. Typically, we set the microwave oscillator at some frequency between 8.2 and 12.4 Gc/sec and varied the magnetic field,  $\vec{H}_{dc}$ , for a maximum echo. The maximum echo always occurred very near the field for free electron cyclotron resonance, within the uncertainty introduced by the inhomogeneity of the magnetic field.

The largest echoes, with a signal-to-noise ratio of  $10^5$ , were observed in a Ne plasma at  $(5-10) \times 10^{-3}$  Torr, an estimated electron density of  $5 \times 10^9/\text{cm}^3$ , and a field inhomogeneity in the plasma of about 0.6%. The magnetic field inhomogeneity improves the time definition of the echo.<sup>1</sup> An oscilloscope picture of a representative echo signal is shown in Fig. 2. One or more secondary echoes (Fig. 2) were observed at the maximum microwave power of 15 W. The strength of the echo signal, representing at maximum  $10^{-2}$  to  $10^{-3}$  of the absorbed incident power, enabled us to vary most of the microwave and plasma parameters over a considerable range while still observing an echo. For this brief note we present only the effect of varying the direction of propagation and those parameters which influence the echo decay constants.

We were able to observe an echo only when

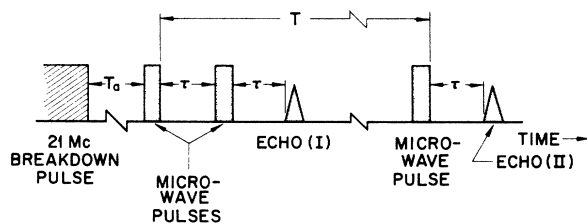


FIG. 1. Schematic representation of the time sequence of breakdown pulse, microwave pulses, and echoes for cyclotron-resonance echo experiment.